Radiographic features of the limbs of juvenile and subadult loggerhead sea turtles *(Caretta caretta)*

Ana Luisa Valente, Ignasi Marco, Maria Angeles Zamora, Maria Luz Parga, Santiago Lavín, Ferran Alegre, Rafaela Cuenca

Abstract

This study aimed to provide the normal radiographic anatomic appearance of the limbs of the loggerhead sea turtle, *Caretta caretta*. Dorsopalmar and dorsoplantar radiographs were taken of the forelimbs and hindlimbs of 15 juvenile and 15 subadult loggerhead sea turtles, 17 alive and 13 dead. For comparison, computed tomographic, gross anatomic, osteologic, and histologic studies were performed on the limbs of 5 of the sea turtles. Bones from the distal part of the fore and hind flippers were seen in detail with a mammographic film–screen combination. The pectoral and pelvic girdles, superimposed by the carapace, were better seen on standard radiographs with the use of rare-earth intensifying screens. Mammographic radiographs of the manus of 5 small juvenile turtles showed active growth zones. Visualization of bone contours in the distal part of the limbs was clearer than in mammals owing to the very few superimpositions. The presence of a substantial amount of cartilage in the epiphyses produced better visibility of limb ends. We conclude that use of a mammography film–screen combination is the best way to evaluate the bony and joint structures of the limbs of sea turtles. Radiography provides reliable images for clinical purposes. Considering the low cost and logistics of this technique, it is a practical ancillary test for marine animal rehabilitation centers to use.

Résumé

L'objectif de la présente étude était de fournir des données sur l'apparence anatomique radiographique normale des membres de la tortue caouanne (Caretta caretta). *Des radiographies dorso-palmaires et dorso-plantaires des membres antérieures et postérieures de 15 tortues caouannes juvéniles et de 15 tortues caouannes sub-adultes ont été prises, 17 d'animaux vivants et 13 d'animaux morts. À titre comparatif, des données de tomodensitométrie, d'anatomie macroscopique et d'études ostéologiques et histologiques ont été obtenues à partir des membres de 5 des tortues marines. Les os provenant de la partie distale des nageoires avant et arrière ont été observés en détails à l'aide d'une combinaison écran–film à mammographie. Les ceintures pectorale et pelvienne, surimposées par la carapace, étaient mieux visualisées sur des films radiographiques standards en utilisant des écrans intensifiant au lanthanide. Des radiographies de la main de 5 tortues juvéniles ont montré des zones actives de croissance. La visualisation du contour des os dans la partie distale des membres était plus claire que chez les mammifères étant donné le peu de surimpositions. La présence d'une quantité substantielle de cartilage dans les épiphyses des membres postérieurs permettait une meilleure visibilité. Nous pouvons conclure que la combinaison film à mammographie–écran est la meilleure méthode pour évaluer les os et les articulations des membres de la tortue caouanne. Les radiographies fournissent des images fiables d'un point de vue clinique. Compte tenu du faible coût et la logistique de cette technique, il s'agit d'un test auxiliaire pratique pouvant être utilisé par les centres de réhabilitation pour mammifères marins.*

(Traduit par Docteur Serge Messier)

Introduction

Sea turtle populations have declined over the past few decades owing to human activity. Boat-strike injuries, entanglement in fishing nets, and the swallowing of hooks, fishing lines, and crude oil are the main causes of sea turtle deaths around the Canary Islands and in the Western Mediterranean (1,2). The loggerhead sea turtle *(Caretta caretta)* is listed as endangered (3) and is the most common species accidentally caught by fishing activities in the Mediterranean Sea. Juveniles and subadults are most commonly caught, and most animals rescued from fishing nets have some degree of limb trauma, which occurs when turtles become entrapped in nets and their extremities are strangulated (2). At rehabilitation centers, proper physical assessment should be performed, as should a minimum standard of blood analysis and radiography (4).

Different imaging methods are available for veterinary practice. However, normal radiologic parameters are scarce for most free-ranging animals, including sea turtles. Previous authors have reported the application of radiologic techniques to reptile species (5–10). However, owing to the wide morphologic variety of reptiles,

Servei d'Ecopatologia de Fauna Salvatge, Facultat de Veterinària, Universitat Autònoma de Barcelona, 08193 — Bellaterra, Barcelona, Spain (Valente, Marco, Lavín, Cuenca); Diagnosis Médica, Córcega, 345, Barcelona, Spain (Zamora); Centre de Recuperació d'Animals Marins; Camí Ral 239, 08330 — Premià de Mar, Barcelona, Spain (Parga, Alegre).

Address all correspondence and reprint requests to Dr. Ana Luisa Valente; telephone: +34 93 581 19 23; fax: +34 93 581 20 06; e-mail: schifinoval@hotmail.com

Received June 20, 2006. Accepted November 22, 2006.

further knowledge of the normal radiographic anatomy in a particular species is required.

This article reports on part of a wide-ranging diagnostic imaging study of the loggerhead sea turtle, its purpose being to present the normal radiographic anatomic appearance of the limbs of the loggerhead sea turtle. We have combined radiologic information with computed tomographic, osteologic, gross anatomic, and histologic data for the appendicular skeleton of this species in order to provide information useful for increasing relevant clinical knowledge.

Materials and methods

Dorsopalmar and dorsoplantar radiographs were taken of the forelimbs and hindlimbs of 15 juvenile and 15 subadult loggerhead sea turtles accidentally caught in pelagic longline sets and fishing nets along the northwestern Mediterranean coast; 17 animals were alive and 13 dead. Juvenile turtles were considered to be those with a minimum straight carapace length (SCLmin) of 21 to 40 cm and subadults those with an SCLmin of 41 to 65 cm (11). The live turtles were temporally housed in the rehabilitation facilities of the Rescue Centre for Marine Animals (CRAM), Premià de Mar, Barcelona, Spain. Only turtles free of limb damage or skeletal abnormalities were considered for this study. The turtles were manually restrained in ventral recumbency, the limbs maintained with adhesive tape in a physiological position. No sedation was required, but the eyes were masked.

Tabletop images were taken with a Rotanode x-ray tube (model E7239; Toshiba Electron Tubes and Devices Company, Tokyo, Japan) at a focal distance of 68 cm. Analog radiography was performed with medical x-ray film used for mammography (UM-MA hc, 24 × 30 cm) and a Fuji AD-MA screen (UM MAMMO fine) and with Super HR-GB film 30 × 40 cm and rare-earth intensifying screens (Fuji ECD), all from Fuji Photo Film Company, Tokyo. With the use of a negatoscope, the radiographs were photographed and digitized at a minimum resolution of 300 dots per inch. The radiographs were evaluated and the anatomic features described when found to be consistent.

Multidetector computed tomography (MDCT) of the whole body was performed in 4 of the juvenile loggerhead sea turtles and in 1 subadult. The turtles were anesthetized with ketamine (Imalgene 1000; Merial, Lyon, France), 15 mg/kg injected intravenously, and diazepam (Almirall Prodesfarma, Barcelona, Spain), 0.5 mg/kg injected into the dorsal cervical sinus to prevent flipper movement. Cardiac frequency was monitored with a Mini-Doppler unit (Doppler High Sensitivity Pocket 112 Doppler D900, Huntleigh Healthcare, Dublin, Ireland), and the animals were carefully kept wet before the scan. A 16-detector-row CT scanner (Aquilion 16; Toshiba Medical, Tokyo, Japan) was used at the following settings: 120 kVp, 250 mA, detector configuration 16 × 1 mm, and matrix 512 × 512. The field of view ranged from 35 to 52 cm, and the total examination took 10 to 15 s, depending on the size of the turtle. The volumetric data for the limbs were reconstructed with a 1-mm slice width and a reconstruction interval of 0.8 mm. Three-dimensional images were generated on a Vitrea computer workstation, version 3.0.1 (Vital Images, Plymouth, Minnesota, USA).

To obtain anatomic information on the limbs of the dead turtles, 5 (2 juveniles and 3 subadults) were frozen at −80°C, and serial parallel sections 18 to 20 mm thick were cut in the dorsal plane with an electric bone saw. The limb bones and associated joints were macroscopically evaluated, and samples of epiphyses of the right humerus, radius, ulna, femur, tibia, fibula, and metacarpal and metatarsal bones and phalanges from digit III were fixed in neutral-buffered 10% formalin solution for histologic study with the use of hematoxylin–eosin stain. The skeletons of 5 loggerhead sea turtles at the Museo de Zoología de Barcelona and the Departamento de Sanitat i Anatomia Animal, Facultat de Veterinària, Universitat Autònoma de Barcelona (UAB), were photographed and radiographed for osteologic data.

Radiologically visible structures were compared with those observed in the osteologic preparations, 3-dimensional (3-D) CT reconstructions, gross anatomic sections, and histologic sections. All radiographic images were analyzed with Adobe Photoshop, version 5.5 (Adobe Systems, San Jose, California, USA); normal and inverted (negative) images were compared.

The anatomic terminology used in this report is that of the *Nomina Anatomica Veterinaria*, as well as specific terminology for sea turtles (12).

Results

Bones from the distal part of the fore and hind flippers were seen in detail in the radiographs obtained with the mammography film–screen combination. The CT-reconstruction images had the best definition for examining cortical bone, density of the matrix, and trabeculae. The pectoral and pelvic girdles were better seen with standard tabletop radiography and rare-earth intensifying screens than with the mammography film–screen combination. These regions will be not described here since they were covered in a previous publication on the coelomic cavity (13). The bones in the juvenile and subadult loggerhead sea turtles did not differ in form or structure; however, some bony features, such as the head and greater tuberosity of the humerus and the head and major trochanter of the femur, were more pronounced in the subadults.

Radiographically, a large joint space was seen in all synovial joints of the limbs (Figure 1A). In the anatomic sections, a thick hyaline cartilage cone plugged each bone forming the greater part of the epiphyseal area (Figure 1B). Mammographic radiographs of 5 small juvenile turtles showed a thin radiolucent line followed by a radiodense, longitudinally striated and thicker band (Figure 2A), mainly in the physes of the metacarpals, metatarsals, phalanges, and distal physes of the humerus. Subchondral growth was observed in all bones. These findings were interpreted on the basis of the histologic analyses for the same animals as active growth zones in the epiphyseal plate (Figure 2D). Long bones consisted primarily of a core of cancellous bone bounded by a thin cortex of compact bone (Figure 2B and 2C). The histologic study carried out in 2 juveniles showed that the epiphysis consisted of a mass of undifferentiated cartilage and a growth zone in which the cells (chondrocytes) of the layer next to the shaft were flattened and arranged in longitudinal columns and showed different degrees of hypertrophy. The chondrocytes nearest the shaft were more vacuolated than those nearest the end of the epiphysis. In the

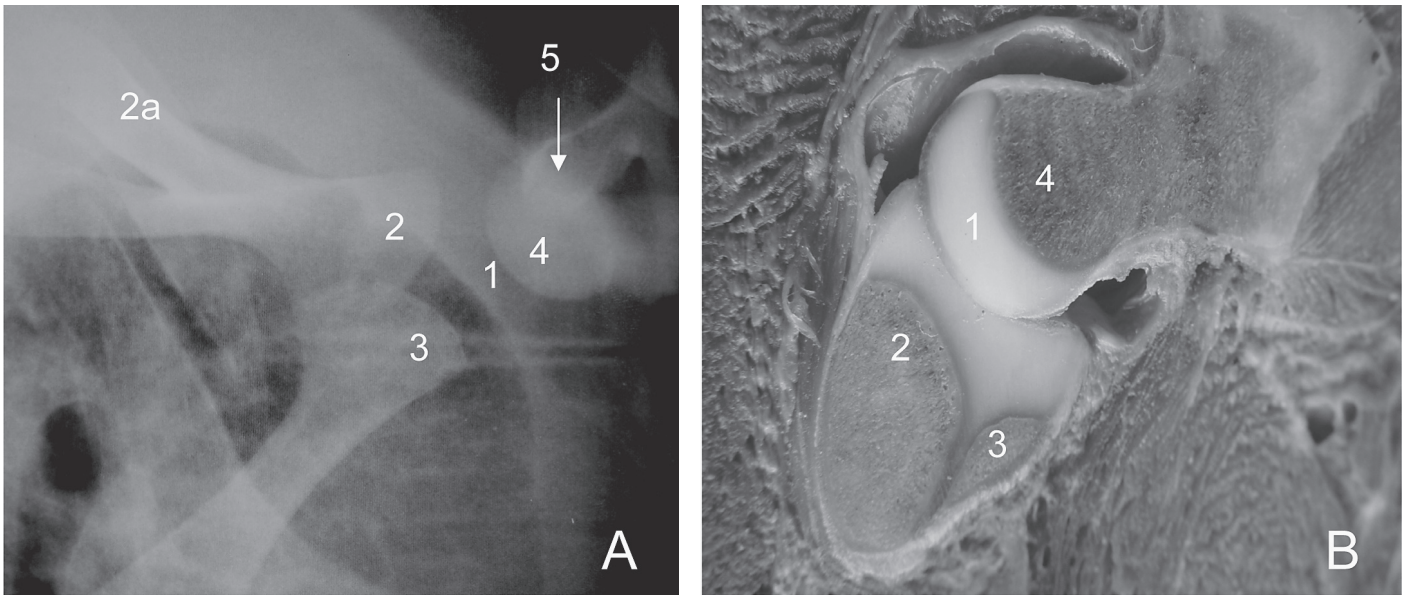

Figure 1. Dorsoventral radiographic view (A) and dorsal anatomic section (B) of the shoulder joint of a loggerhead sea turtle. A: 1 — cartilaginous part of the humerus head; 2 — articular end of the scapula; 2a — acromion process (cranial fused bone); 3 — articular end of the coracoid; 4 — humerus head; 5 — greater tuberosity.

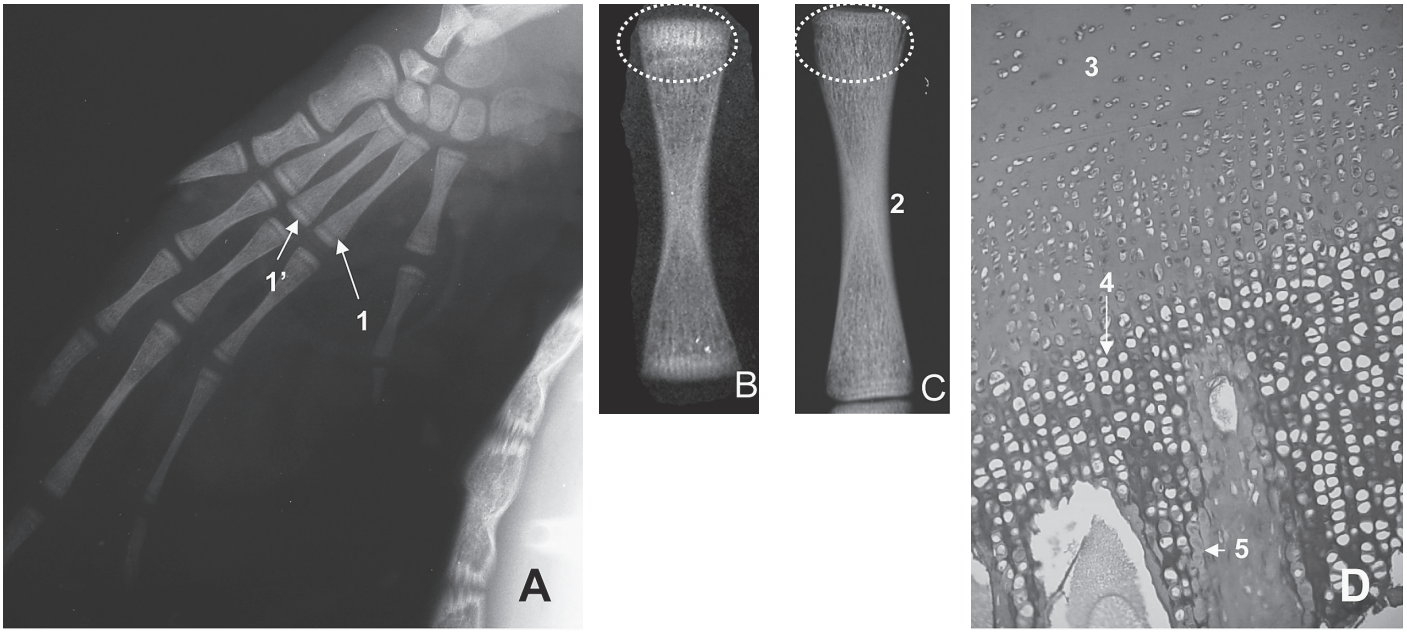

Figure 2. Dorsoventral radiographic view (A) of the manus of a small juvenile loggerhead sea turtle. Close-ups of the proximal phalanx of digit II of juvenile (B) and subadult (C) specimens. Histologic survey of the growth area (D) with the use of hematoxylin–eosin stain; magnification, ×100. 1 — epiphyseal growth zone; 1' — epiphyseal plate; 2 — ossified diaphysis; 3 — undifferentiated cartilage; 4 — longitudinal columns of hypertrophied chondrocytes; 5 — mineralization of cartilage template of endochondral bone.

3 subadult turtles, the cellular arrangement in the growth area was similar to that observed in the 2 juvenile turtles; however, the longitudinal columns were not so well defined. In all cases, mineralization of a cartilage template was observed, and endochondral bone was set down on the eroded surface of the cartilage (Figure 2D).

Humerus

The proximal epiphysis of the humerus was not clearly seen radiographically owing to superimposition of the carapace and plastron bones. The head of the humerus was seen joined with the articular surface formed by the scapula, acromion, and coracoid bones (Figures 1 and 3A). Caudal to the head, the great and rounded medial process (greater tuberosity) was easily identified in all radiographs (Figures 3A and 3C). Morphologically, this structure was radiographically similar to the head of the humerus in both juvenile and subadult turtles (Figures 3A and 3B). However, in CT images and in osteologic and anatomic dissections, the greater tuberosity was more prominent than the head (Figure 3C). A large fossa could be clearly seen in the radiographs as a radiolucent area immediately below the head and the greater tuberosity. The deltoid crest could be

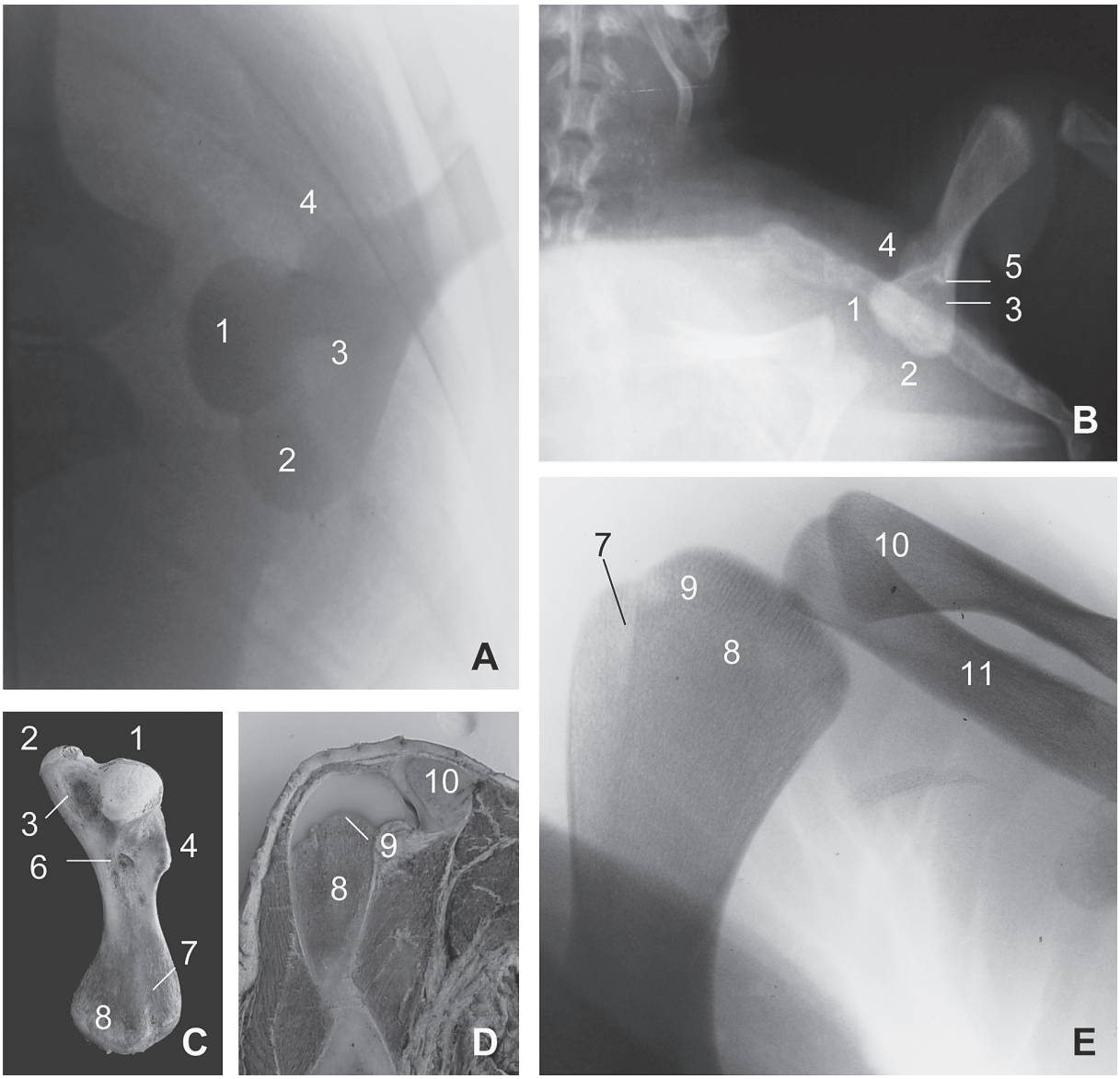

Figure 3. Negative image of dorsoventral radiographic views of the humerus of subadult (A, E) and juvenile (B) loggerhead sea turtles, ventral view of the humerus (C), and anatomic section of the elbow joint (D). 1 — humerus head; 2 — greater tuberosity; 3 — fossa between the humerus head and the greater tuberosity; 4 — deltoid crest; 5 — sharp process on the deltoid crest; 6 — nutrient foramen; 7 — intercondylar sulcus; 8 — medial condyle; 9 — growth zone; 10 — radius; 11 — ulna.

identified as a rounded projection of the bone contour on the cranial border of the humerus (Figures 3A to 3C). In 3 subadult turtles, this crest was more prominent than in juveniles and, depending on the rotation of the limb at the moment of the examination, the structure was seen partially superimposed on the humeral head (Figure 1A). In 1 juvenile turtle, a sharp process was seen on the caudal border of the crest (Figure 3B). The nutrient foramen on the ventral surface of the humerus (Figure 3C) could not be observed in all radiographs. In the distal epiphysis of the humerus, the medial and lateral condyles were recognizable owing to the groove between them (Figures 3C and 3E).

Radius and ulna

The bones were seen partially superimposed, the radius (shorter than the ulna) being seen cranial to the ulna. The radius was seen to have a broad and triangular proximal epiphysis and a concave caudal border. The distal end of the straight and tubular ulna was superimposed on the ulnare and radiale carpal bones (Figures 3E and 4A). No pronounced processes or grooves were visualized in either bone. The cortices were markedly thickened in the mid-diaphyseal region but tapered proximally and distally (Figures 3E and 4A).

Carpal bones

The 9 carpal bones could be clearly recognized in the carpus owing to scant superimposition (Figure 4). In the proximal row, the radiale was seen as a rectangular bone placed laterally and the ulnare as semilunar, with a great curvature pointed medially; the pisiform stood out medially from the distal row. The small and rounded centrale bone was seen immediately ventral to the radiale and ulnare

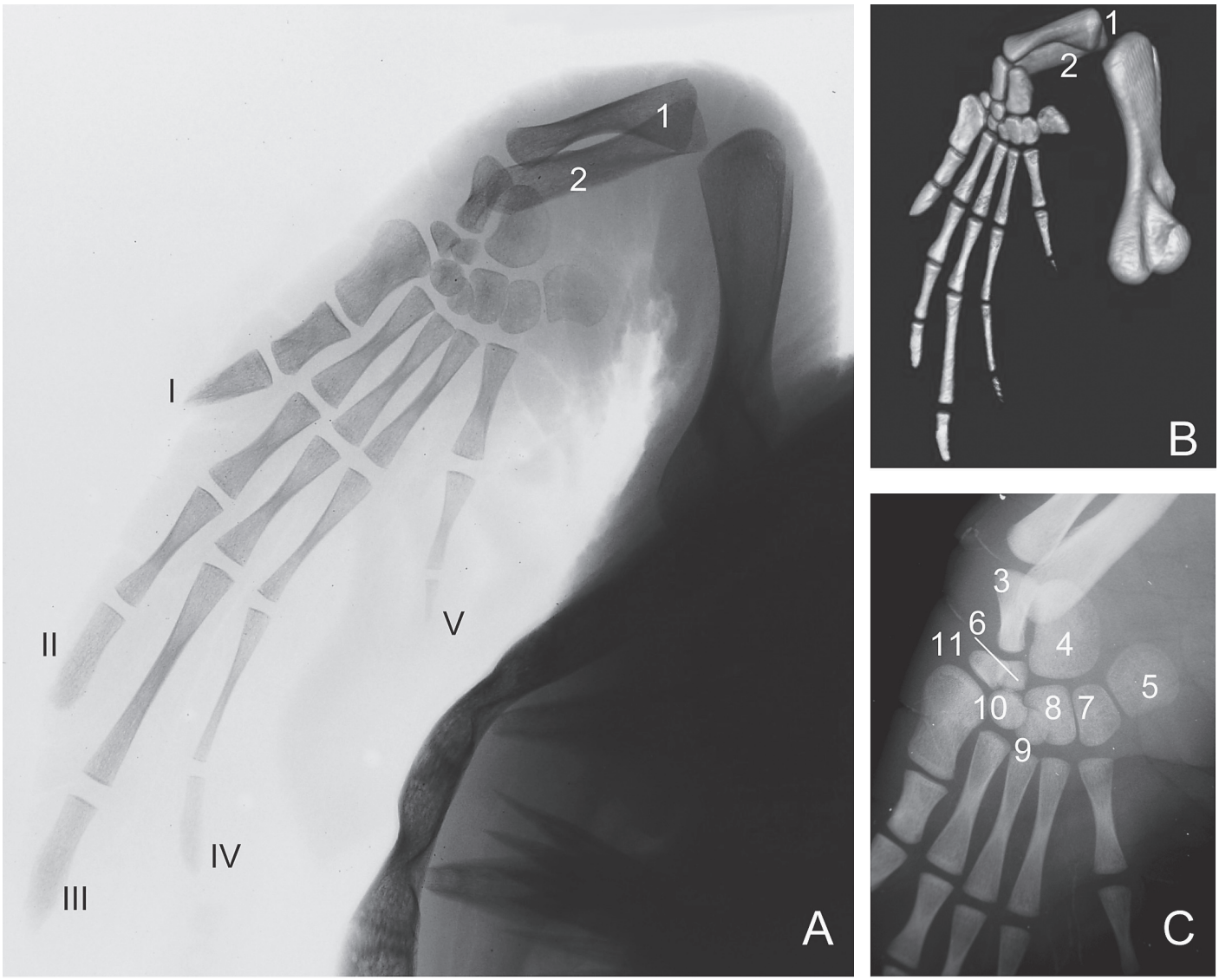

Figure 4. Negative image of a dorsoventral radiographic view (A) and a 3-dimensional (3-D) reconstruction (B) of the manus of a juvenile loggerhead sea turtle, with a close-up of the radiographic view of the carpal region (C). 1 — radius; 2 — ulna; 3 — radiale; 4 — ulnare; 5 — pisiform; 6 — centrale; 7 to 11 — other carpal bones. Roman numerals indicate the respective digits.

bones. In the distal row of the carpus, 5 carpal bones were identified, each respective to a digit (Figure 4C).

Metacarpals and phalanges

The metacarpal bones and phalanges were seen to have similarly shaped digits except for digit I, which has a flattened articular surface on the physis and an elongated, thin diaphysis. Digit I is prominent and consists of a short and strong metacarpal bone and 2 sturdy phalanges, proximal and distal (Figure 4A). Digit II has a shorter and thicker proximal phalanx than do digits III and IV. The intermediate phalanx of digit III is the most slender and the longest of all. Digit V has only 2 phalanges. In the radiographs and the CT images, no sesamoid bones were seen in association with the flipper joints (Figures 4A and 4B).

Femur

The joint between the head of the femur and the acetabulum superimposed on the carapace bones was clearly visible in all the radiographs taken with conventional plain film (Figure 5A and 5B). In juvenile turtles, most of the head is made up of cartilage. In subadult animals, the head is ossified, stouter than that of the juveniles, and joined to the physes through a thick neck (Figure 5). The prominent major trochanter was seen caudal to the head. The diaphysis is long and slender. The condyles on the distal epiphyses could not be differentiated because of superimposition on the marginal bones of the carapace. Neither the patella nor other sesamoid bones were visualized in the stifle joint (Figures 5A and 6B).

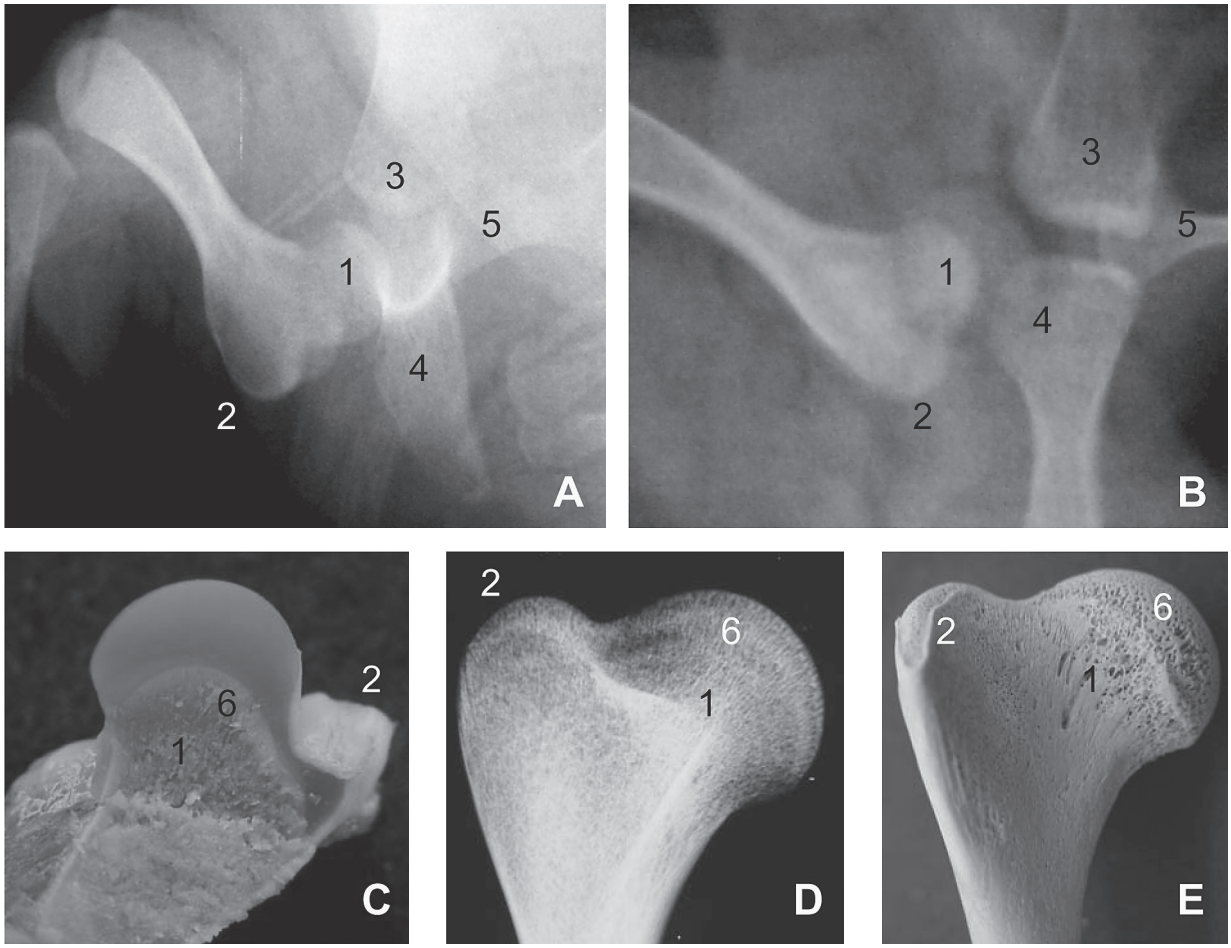

Figure 5. Dorsoventral radiographic views of the hip joint of subadult (A) and juvenile (B) loggerhead sea turtles. Anatomic section (C), radiographic view (D), and osteologic preparation (E) of the proximal epiphysis of the femur. 1 — femoral head; 2 — greater trochanter; 3 — pubis; 4 — ilium; 5 — ischium; 6 — growth zone.

Tibia and fibula

The tibia and fibula could be seen with scant superimposition of epiphyses. The tibia is thicker and cranial to the fibula and has a convex articular surface at the proximal epiphysis. Both bones are elongated and fairly similar in length (Figures 6A and 6B).

Tarsal bones

Six tarsal bones were perfectly visualized in all radiographs. We identified 2 rounded and bigger bones and 4 quite spherical and smaller bones (Figure 6). In the proximal row, the great astragalus was seen laterally below the tibia, and the calcaneum was seen as a small, rounded bone medially below the fibula (Figure 6C). In the distal row, the tarsal bone of digit V, which articulates with the metatarsal bones of digits IV and V, is prominent because of its heart shape and large size relative to that of the other tarsal bones, which are spherical and just proximal to the respective digits, I, II, and III (Figure 6C).

Metatarsals and phalanges

Similar to the forelimb, digit I of the hindlimb consists of a short, flattened, and strong metatarsal bone and 2 sturdy phalanges. Digits II to V have 3 somewhat proportional phalanges. The metatarsal bone of digit V is flattened and resembles that of digit I, although the former is slightly smaller (Figures 6A and 6B).

Discussion

Routine radiography of the limbs is usually performed in at least 3 views: dorsopalmar (or dorsoplantar), lateral, and oblique (14). The flattened shape and relative thinness of the loggerhead sea turtle's flippers when compared with the compact and quite cylindrical limbs of terrestrial vertebrates preclude the use of other views. Distortion in size or shape was observed only at the proximal end of the humerus, where the great tuberosity was partially superimposed on itself, creating an unrealistic shape.

The numerous anatomic differences between the limbs of chelonians and mammalians, and even between turtles and other reptiles, make sea turtles unique patients. Because of the scant superimpositions between bones, the contours are more clearly visualized in radiographs of the limbs of sea turtles than in those of mammals, such as dogs and cats. Additionally, the massive amount of cartilage in the epiphyses produces better visibility of the articular ends. These cartilaginous epiphyses become gradually thinner with age because

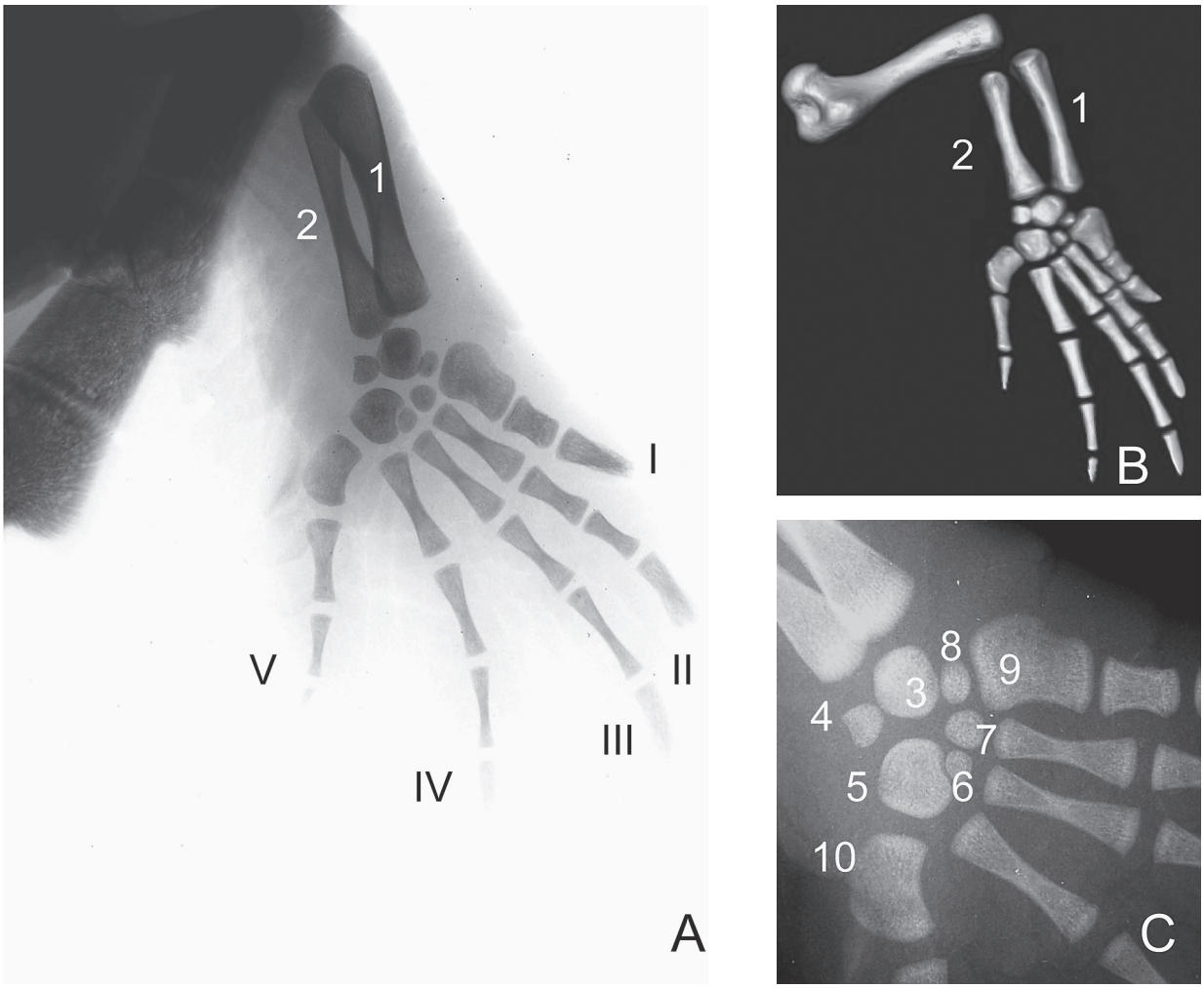

Figure 6. Negative image of a dorsoventral radiographic view (A) and 3-D reconstruction (B) of the pedis of a juvenile loggerhead sea turtle, with a close-up of the radiographic view of the tarsal region (C). 1 — tibia; 2 — fibula; 3 — astragalus; 4 — calcaneum; 5 — tarsal bone V; 6, 7, and 8 — other tarsal bones; 9 — metatarsal bone from digit I; 10 — metatarsal bone from digit V.

undifferentiated cells pass into the growth zone, and, consequently, the articular and growth zones come into close approximation; however, growth may be retained even in aged animals (15). Easy visualization of the bone ends has practical clinical application, because the diagnosis of bone disorders such as fractures, osteomyelitis, and osteofibrosis, along with many joint abnormalities, could easily be made with a conventional and inexpensive radiographic technique.

Previous studies (8) have reported that the matched mammography film–screen combination is superior to standard bucket and tabletop radiography in the evaluation of the bones and soft tissues of small reptiles. The combination results in a resolution of 10 to 20 line pairs (lp)/mm, as opposed to 5 to 10 lp/mm with standard radiographic techniques (8), which in this study permitted optimal visualization of the cancellous and compact bone arrangement in the long bones, as well as the epiphyseal growth areas. The growth areas observed in our animals as a radiopaque band at the end of the long bones were also observed in skeletally immature humans (16): after a temporary slowdown or cessation of rapid longitudinal bone formation, transverse trabecular bands of increased radiodensity appeared; when growth rates were normal, longitudinally oriented trabeculae with interspersed marrow elements predominated at the zone of transformation of cartilage to bone.

Radiologic examination of the long bone epiphyses, together with evaluation of time of closure, has been used as a chronologic reference in various species of vertebrates (17,18). In reptiles, this methodology is not suitable because endochondral growth may be life-long (15). On the other hand, turtles and crocodiles do not have isolated ossification centers in the epiphysis, such as occurs with squamates (snakes and lizards) and mammals (15). Curiously, in our study, epiphyseal plates were detected radiographically in the long bones of the manus in only 5 of the 15 juvenile turtles. We are unaware of the reasons why these areas were not seen in all the juvenile animals, as would be expected. Patterns of reptile growth have attracted considerable attention over the past few decades (19–21). Growth rings in the transverse section of the humerus have been studied in reptiles, including sea turtles (22), as a method of calculating age. Turtles grow at different rates during the ontogenetic period, the rate being influenced by the quality and quantity of the diet (15,23). In the early years of life, oceanic-stage loggerhead sea turtles have relatively little control over their geographic position or movements and thus have an extremely stochastic lifestyle, with

great variation in food availability and temperature (24). Temporary cessation of growth may occur even in relatively young turtles; growth is resumed later, after perforation of the bony plates and renewal of activity by the marrow (15). The environmental variation results in variable growth rates, which could be directly associated with the inconsistent presence of a distinct growth area in the long bones of juvenile turtles, as found in this study.

The shape and structure of bones is governed by many factors — genetic, metabolic, and mechanical. In chelonians, the pectoral and pelvic arches appear to have a very anomalous position, inasmuch as they seem to be situated inside and not outside the skeletal trunk (12). Modification of the sea-turtle pectoral limb into a semi-rigid, elongated, and flattened flipper for forelimb propulsion has resulted in proportional changes in the limb skeleton and shifts in the distributions of muscle tissue (25). The reduced presence of musculoskeletal elements accounts for the absence of sesamoid bones noted in the radiographs of this study. Although reptilian compact bone is similar to the compact bone of other vertebrates, we found the bone cortex to be thinner in the sea turtles, with minor radiographic contrast between bones. Compared with well-known species such as the dog and cat (26), turtles in general seem to have a smoother diaphyseal surface, without pronounced processes, crests, or tuberosities. As a result, there is a clearer radiographic image of the bone's internal structure, with minimal superimposition of superficial bony elements. The response pattern of the bone to injury in reptiles differs significantly from that in mammals. In reptiles, new periosteal bone production is less prominent, and it is common to see a radiolucent fracture line in clinically stable fractures that have healed with a fibrous callus (10,27).

Mammographic radiography and multiplanar CT reconstruction were observed in this study to provide similar information. The latter costs more, involves a technique not readily available in rehabilitation centers, and requires more time for image manipulation. Three-dimension reconstruction was useful to show different views of the structures. However, this kind of virtual processing, when applied to extremely tight bone structures, as is the case with carpal and tarsal bones, may produce an artificial effect whereby the structures seems to be joined.

We conclude that the mammographic film–screen combination is the best radiographic modality for evaluating the bone and joint structures of the forelimbs and hindlimbs of juvenile and subadult sea turtles. Radiography provided reliable images for clinical purposes. Considering the low cost and logistics of this technique, it is one of the more practical ancillary tests that marine animal rehabilitation centers can use.

Acknowledgments

We thank Professor Francisco Reina and laboratory technician Isabel Delgado Calvarro, Facultat de Medicina, UAB, for help with the anatomic sections, as well as radiodiagnostic technician Montse March for technical support with the MDCT. Thanks also go to the Museo de Zoología de Barcelona and the Departamento de Sanitat i Anatomia Animal, Facultat de Veterinària, UAB, for providing the turtle skeletons. We are grateful to Dr. Jordi Franch, Departamento de Medicina i Cirugia Animal, Facultat de Veterinària, UAB, for reviewing the manuscript.

References

1. Orós J, Torrent A, Calabuig P, Déniz S. Diseases and causes of mortality among sea turtles stranded in the Canary Islands, Spain (1998–2001). Dis Aquat Organ 2005;63:13–24.
2. Pont SG, Alegre FN. Work of the Foundation for the Conservation and Recovery of Marine Life. Marine Turtle Newsl 2000;87:5–7.
3. International Union for Conservation of Nature and Natural Resources, Species Survival Commission. 2006 Red List of Threatened Species. Available at www.iucnredlist.org (accessed 2006 Feb 22).
4. Wyneken J, Mader DR, Weber III ES, Merigo C. Medical care of sea turtles. In: Mader DR, ed. Reptile Medicine and Surgery. St. Louis, Missouri: Saunders Elsevier, 2006:972–1007.
5. Wyneken J. Computed tomography and magnetic resonance imaging anatomy of reptiles. In: Mader DR, ed. Reptile Medicine and Surgery. St. Louis, Missouri: Saunders Elsevier, 2006: 1088–1096.
6. Rübel A, Kuoni W. Radiology and imaging. In: Frye FL, ed. Biomedical and Surgical Aspects of Captive Reptile Husbandry. 2nd ed. Melbourne, Florida: Krieger Publishing, 1991:185–208.
7. Jackson OF, Sainsbury AW. Radiological and related investigations. In: Beynon PH, ed. Manual of Reptiles. Quedgeley, England: British Small Animal Veterinary Association, 1992: 63–72.
8. DeShaw B, Schoenfeld A, Cook RA, Haramati N. Imaging of reptiles: a comparison study of various radiographic techniques. J Zoo Wildl Med 1996;27:364–370.
9. Hernandez-Divers S, Hernandez-Divers S. Diagnostic imaging of reptiles. In Practice 2001;23:370–391.
10. Wilkinson R, Hernandez-Divers S, Lafortune M, Calvert I, Gumpenberger M, McArthur S. Diagnostic imaging. In: McArthur S, Wilkinson R, Meyer J, eds. Medicine and Surgery of Tortoises and Turtles. Victoria, Australia: Blackwell Publishing, 2004:187–238.
11. Dodd CK Jr. Synopsis of the Biological Data on the Loggerhead Sea Turtle Caretta (Linnaeus 1758). US Fish and Wildlife Service Biological Report 1988;88(14):35–82.
12. Wyneken J. The Anatomy of Sea Turtles. US Department of Commerce NOAA Technical Memorandum NMFS-SEFSC 2001;470:43–58.
13. Valente AL, Cuenca R, Parga ML, Lavín S, Franch J, Marco I. Cervical and coelomic radiologic features of the loggerhead sea turtle, *Caretta caretta*. Can J Vet Res 2006;70:285–290.
14. Morgan JP. Techniques of Veterinary Radiography. Ames, Iowa: Iowa State University Press, 1993:113–168.
15. Haines RW. Epiphyses and sesamoids. In: Gans C, d'A Bellairs A, eds. Biology of the Reptilia. New York, New York: Academic Press, 1969:81–115.
16. Ogden JA. Growth slowdown and arrest lines. J Pediatr Orthop 1984;4:409–415.
17. DiGiancamillo M, Rattegni G, Podestà M, Cagnolaro L, Cozzi B, Leonardo L. Postnatal ossification of the thoracic limb

in striped dolphins *(Stenella coeruleoalba)* (Meyen, 1833) from the Mediterranean Sea. Can J Zool 1998;76:1286–1293.
18. Serrano E, Gállego L, Pérez JM. Ossification of the appendicular skeleton in the Spanish Bies *Capra pyrenaica* Schinz, 1838 (Artiodactyla: Bovidae), with regard to determination of age. Anat Histol Embryol 2004;33:33–37.
19. Hailey A, Coulson IM. The growth pattern of the African tortoise *Geochelone pardalis* and other chelonians. Can J Zool 1999;77:181–193.
20. Bjorndal KA, Bolten AB, Martins HR. Somatic growth model of juvenile loggerhead sea turtles *Caretta caretta:* duration of pelagic stage. Mar Ecol Prog Ser 2000;202:265–272.
21. Arcos-García JL, Peralta MAC, Rosales VHR, Martínez GDM, Cerrilla MEO, Sánchez FC. Growth characterization of black iguana *(Ctenosaura pectinata)* in captivity. Vet Mex 2002;33: 409–419.
22. Zug GR, Wynn A, Ruckdeschel C. Age estimates of Cumberland Island loggerhead sea turtles. Marine Turtle Newsl 1983;25: 9–11.
23. Spencer RJ. Growth patterns of two distributed freshwater turtles and a comparison of common methods used to estimate age. Aust J Zool 2002;50:477–490.
24. Bjorndal KA, Bolten AB, Dellinger T, Delgado C, Martins HR. Compensatory growth in oceanic loggerhead sea turtles: response to a stochastic environment. Ecology 2003;84:1237–1249.
25. Wyneken J. The external morphology, musculoskeletal system, and neuro-anatomy of sea turtles. In: Lutz PL, Musick JA, Wyneken J. The Biology of Sea Turtles. Vol 2. Boca Raton, Florida: CRC Press, 2002:39–77.
26. Konde LJ. Appendicular skeleton — companion animals. Diseases of the immature skeleton. In: DE Thrall, ed. Textbook of Veterinary Diagnostic Radiology. Philadelphia, Pennsylvania: WB Saunders, 1994:94–104.
27. Silverman S. Diagnostic imaging. In: Mader DR, ed. Reptile Medicine and Surgery. St. Louis, Missouri: Saunders Elsevier, 2006:471–489.